Solar Energy Materials and Solar Cells 185 (2018) 233–239

Contents lists available at ScienceDirect

Solar Energy Materials and Solar Cells

journal homepage: www.elsevier.com/locate/solmat

CSP mirror soiling characterization and modeling

Ricardo Conceição[a,b,*], Hugo G. Silva[a,b], Manuel Collares-Pereira[a,b]

[a] Renewable Energies Chair, University of Évora, Portugal
[b] Institute of Earth Sciences, University of Évora, Portugal

ARTICLE INFO

Keywords:
Solar energy
CSP
Soiling
Modeling

ABSTRACT

Soiling stands as a major problem for solar energy conversion technologies, causing unwanted transmittance, reflectance and absorbance losses. In this paper, a TraCS (Tracking Cleanliness Sensor) is used to quantify soiling effect in a flat mirror and to calculate soiling rates between periods without rain. Environmental parameters such as vertical wind speed, air temperature, relative humidity and particulate matter in the atmosphere are used as predictors to model soiling. Relations and trends between input and output are analyzed using a simple linear regression model and also through an interaction model. Further investigation is performed with a neural network approach to assess its viability for this type of problem and also for comparison with the previous models.

1. Introduction

Soiling, the process of atmospheric particle settling on surfaces, is a general problem and leads to the need of cleaning, e.g. glass windows of skyscrapers, house cleaning, and nonetheless it is an obstacle for solar conversion technologies [1–7]. It is known that soiling is mostly a local phenomenon, which depends on with the amount of particles suspended in the atmosphere, as well as on environmental conditions. The rural region of Évora, Alentejo, Portugal (Southern Europe), has been under study regarding the effect of soiling in PV technology. The most severe seasons for soiling were identified [7], as well as occasional non-local effects [6]. However, there is a lack of studies regarding the effect of soiling in CSP compared to PV and none for this region or other similar rural areas, which provides a unique research opportunity. The direct effect of soiling in PV production is easier to investigate than in any CSP technology, due to it intrinsic simplicity. This is one of the reasons why CSP soiling studies are more scarce. It should be noted that measurements of mass accumulation and transmittance/reflectance losses on glass/mirror samples (in a static position, which is usual) can be used as in PV technology related results. However, a more realistic CSP study, might require samples to move throughout the day, to simulate the tracking associated with such systems. Despite this, there are already interesting studies about CSP soiling [8–11]. Additionally, a higher soiling impact is expected in CSP than PV, due to the fact that light goes twice through the soiling layer, which can lead to more scatter and therefore less useful irradiance (given the small acceptance angles of the concentrators). In fact, soiling will modify the light path, not only when it reaches the mirrors, but also as it exits them and also increase the internal reflections within the glass. Overall, this process will result in a soiling effect which is 5–10 times worst than in PV [12].

It is the goal of this paper to develop soiling prediction models using three different methods: (i) linear, (ii) linear with interaction terms and (iii) a neural networks type. The prediction of soiling has been shown to be very difficult, mainly because it is essentially an atmospheric process, which usually needs to take into account many environmental parameters, which makes the problem complex. The analysis will start with a linear relationship to assess variable's trends. A linear regression will also be tested with interaction terms to check if there is any relation between the output and interlinked predictors. However, since the process may be very complicated to solve explicitly, a neural network with 1 hidden layer was designed and the optimum number of neurons calculated through a similar process as in [13]. The objective is not only to try to find different models that fit the data well and can serve as prediction models, but also to evaluate possible trends and relations between the variables, which can be explained from a physical point of view.

2. Soiling effect and environmental measurements

2.1. Measurements setup

Measurements of soiling effect on mirror reflectance were performed using a TraCS from CSP Services (Germany) mounted on a SOLYS 2 sun tracker, from Kipp & Zonen (Holland, uncertainty ≤ 2% for pyrheliometer hourly values); vertical wind speed was retrieved using a WindMaster Pro 3-Axis Anemometer from Gill Instruments (UK,

* Corresponding author at: Renewable Energies Chair, University of Évora, Portugal.
E-mail address: rfc@uevora.pt (R. Conceição).

https://doi.org/10.1016/j.solmat.2018.05.035
Received 2 March 2018; Received in revised form 10 May 2018; Accepted 15 May 2018
0927-0248/ © 2018 Elsevier B.V. All rights reserved.

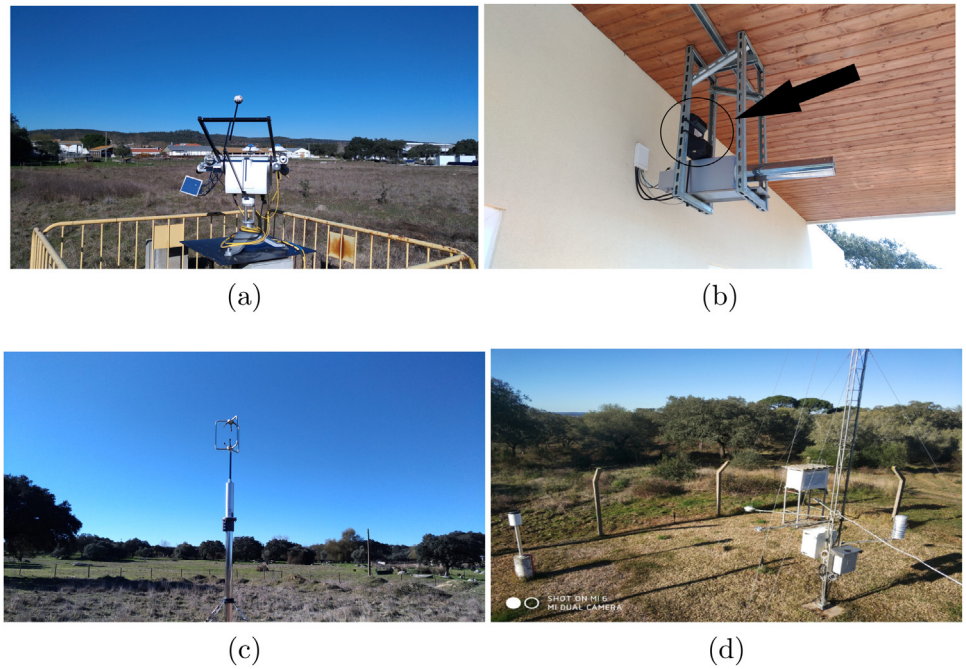

Fig. 1. Measuring instrumentation: (a) TraCS and SOLYS2; (b) Dylos DC1100 Pro; (c) WindMaster Pro; (d) Meteorological station.

uncertainty ≤ 1.5% RMS); particulate matter measurements were taken with a DC1100 Pro from Dylos Corporation (USA, uncertainty ≤ 10%); temperature, relative humidity and precipitation were measured at a nearby meteorological station (≈ 750 m) with a Thermo-Hygrometer (Thies Clima, Germany, with uncertainty ≤ 3% for relative humidity and 0.5 °C for temperature) and a Tipping Bucket Rain gauge from RM Young (USA, uncertainty ≤ 2%), respectively. Below, in Fig. 1, are presented the instruments referred before:

It should be noted that soiling effect is calculated through comparison between the direct normal irradiance, I_b, and the irradiance measured by a second pyrheliometer, I_b^r, reflected by the TraCS's mirror [14,15]. This mirror is rotating and performs a full revolution every 10 min and due to the fact that sun spectrum is variable throughout the day, daily means were calculated using data around solar noon. This process will be explained afterwards.

2.2. Soiling index

The measurement campaign started in June 2017 and lasted until the end of that year. The mirror was cleaned at the beginning of every month from June to August and then left untouched, due to the start of the raining season. During Summer, cleaning was performed to avoid soiling saturation, above which no measurements could be done.

The soiling index, λ, here defined as the normalized ratio between the reflected direct normal irradiance, I_b^r, from the mirror and measured direct normal irradiance, I_b. The soiling index is represented in Fig. 2a and given by:

$$\lambda = 1 - \frac{\rho}{\rho_0}, \tag{1}$$

where $\rho = \frac{I_b^r}{I_b}$. The parameter ρ_0 corresponds to the maximum weighted reflectance measured with the mirror cleaned. This value was calculated by the manufacturer after a series of tests and represents the clean scenario mean reflectance.

The outcome of Eq. (1) is a null value in the absence of soiling, and as the particle deposition increases the soiling index also increases.

The effect of manual cleaning done to the mirror until September can be observed. It should be noted that the results derived from cleaning are not always the same, probably due to improper cleaning, as well as slight changes in mirror positioning, which can influence the irradiance that strikes the pyrheliometer. However, for this study, relative values are more important than absolute ones, since the soiling of the next day will be compared to the previous one.

Regarding the data, it is seen that Summer is indeed the worst season for soiling; perhaps an exception should be made for Spring (the sensor was not working yet), when high soiling values were detected for PV technology [7]. Later, in November and December, after rain and dew formation has been detected regularly (more than during Summer), λ recovered to low values.

2.3. Environmental parameters and methodology

Daily means were calculated following the schematic in Fig. 3. Two different days are represented, where the yellow curve corresponds to typical TraCS measurements. The mean of the soiling index of the day before is represented by λ_i, while for the next day it is given by λ_{i+1} and it is calculate around solar noon, represented by the black lines. The difference between the previous day and the next day is represented by $\Delta\lambda$, see Eq. (2).

$$\Delta\lambda = \lambda_{i+1} - \lambda_i \tag{2}$$

This parameter represents an increase of soiling from one day to the following, if it is positive, and a reduction of soiling, if it is negative. Particulate matter values, $PM_{0.5-2.5}$, correspond to a 24-h mean, from 14 h of the previous day to the next day, as well as vertical wind speed, VWS. Temperature, T, and relative humidity, RH, are a result of the mean from 9 h of the previous day until 6 h of the next day, see Fig. 3. Since $PM_{0.5-2.5}$ measurements have no RH compensation, all $PM_{0.5-2.5}$ values (minutely scale) corresponding to RH above 65% were removed, which implies that for some nights there are possibly no data for a few hours. To characterize the night period, both T and RH were used, which are also important for dew formation phenomenon, as well as hygroscopic growth [16]. Periods with precipitation were removed, since it is seen that is has a cleaning effect and the interest here is to study other environmental parameters that are possible interlinked with soiling effect.

Environmental parameters are presented in Fig. 4. It can be seen that the particulate matter, in Fig. 4a, which represents particulate

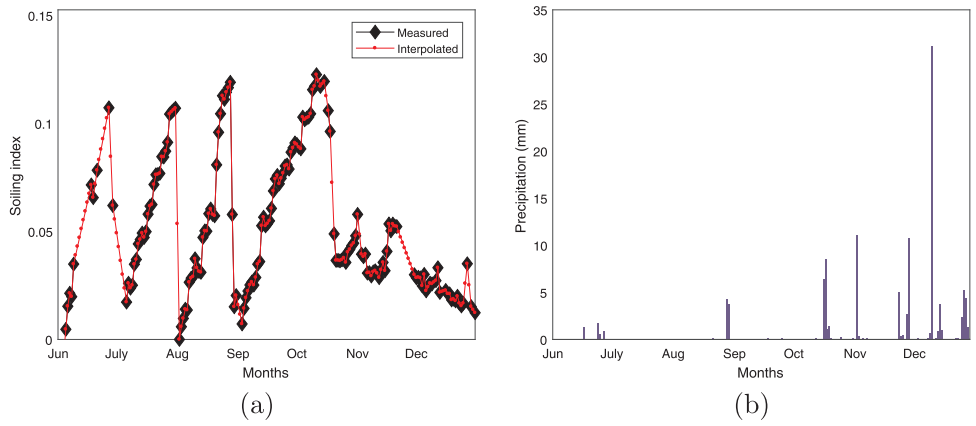

Fig. 2. (a) Soiling index; (b) Precipitation.

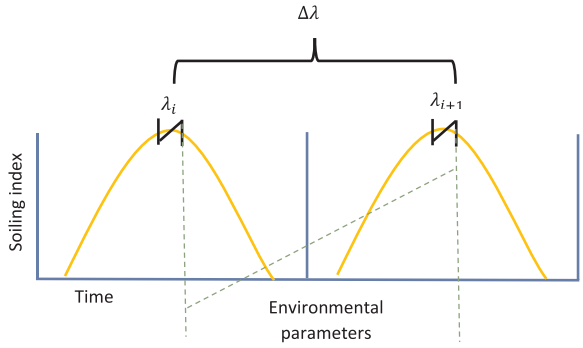

Fig. 3. Calculation process schematic.

matter between 0.5 and 2.5 μm, is rather constant throughout the campaign, excluding peaks towards Fall, which are due to agricultural activities (more intensive during that season). The parameter *VWS*, present in Fig. 4b, is mostly negative, pointing downwards, and with higher intensity during Summer compared to Fall, which likely indicates higher strong and dry convection [17]. It should be noted that *VWS* corresponds to the vertical component of the air direction, which means that its positive velocity means pointing upwards while a negative value means pointing downwards. During Summer, *T*, presented in Fig. 4c, is higher compared to other seasons, as expected, while *RH*, presented in Fig. 4d, has high values during the whole campaign, however what is observed from Summer to Fall is the fact that these tend to increase in frequency, which is understandable, since Summer days are dryer.

3. Soiling modeling and prediction

3.1. Multiple linear regression model

The data for this model and the subsequent models is always the same. The mean of the environmental parameters that will be related with $\Delta\lambda$, for the different models, is derived as referred before.

A stepwise regression method was used, which is based in adding/removing terms in a relation between predictors in order to achieve to maximize some criterion. The criterion used for adding or removing terms is the Adjusted R-Squared, $adjr^2$, since the r^2 will always increase if more related terms are added.

The inputs, for all models, are: $PM_{0.5-2.5}$, $PM_{0.5}$ (which stands for particulate matter above 0.5 μm), *VWS*, *T* and *RH*. The output $\Delta\lambda$ of the multiple linear regression (MLR) model is given by:

$$\Delta\lambda = \beta_0 + \beta_1 X_1 + \beta_2 X_2 + \ldots \beta_n X_n \quad (3)$$

The stepwise method begins with only a constant term (intercept) and follows towards a linear model, testing combinations of variables and finalizes with the one that maximizes the $adjr^2$. For this particular model, only four inputs provide such combination: $PM_{0.5-2.5}$, *VWS*, *T*, and *RH*. Such model has the following statistical parameters: $r^2 = 0.150$, $adjr^2 = 0.121$ and $RMSE = 0.0045$. The corresponding equation for these predictors is shown in Eq. (4). The fact that $PM_{0.5}$ is not chosen as a variable that contributes to the model, has two causes: the mutual correlation of $PM_{0.5}$ and $PM_{0.5-2.5}$, which excludes one of these variables from the relation; smaller particles have a higher scattering effect than large ones [8].

$$\Delta\lambda_{MLR} = \beta_0 + \beta_1 PM_{0.5-2.5} + \beta_2 RH + \beta_3 T + \beta_4 VWS \quad (4)$$

Increased relative humidity has a positive impact on the output, which was also detected in [18]. This can be explained by the fact that hygroscopic growth starts to take place for high values of relative humidity [16,19], which increases the water contend of some aerosol species, making them more prone to settling [20]. Two different reasons may also exist which are: if the relative humidity is high enough there can be dew formation, which can trap particles more easily through capillary forces [21], however if the amount of dew formed is very high, it is more likely to clean the surface; if there is no dew formation but there is an excess of water molecules aggregated to particles, that may enhance the electrostatic adhesion to surface since water molecules are bipolar.

Higher air temperatures are also connected to more soiling. In this context, higher air temperatures are connected to Summer days, while lower values are connected to Fall. As seen in Fig. 2a, soiling is higher during Summer and so are temperatures, which means that this output and input are seasonally connected. This matter will be deepened afterwards. Vertical wind speed has a positive effect on soiling, which means that enhances it when pointing downwards, increasing particle deposition.

As expected, such linear model is not complex enough to explain how these variables may be related with the loss/gain of soiling from one day to the other. Such model has been studied by others [18,22], with a $r^2 = 0.167$, which is a similar value to the one found here. However, it should be noted that Guo and co-workers obtained this value using 10 variables, which means that using only 4 would certainly lead to a lower r^2.

3.2. Multiple linear regression of interaction terms model

Previous analysis shows that using a simple linear model is not enough to explain $\Delta\lambda$ and most likely the predictors are connected to each other, since dust deposition and re-suspension are processes that may depend on such combinations. A multiple linear regression model of interaction terms, MLRIT, is now considered as follows:

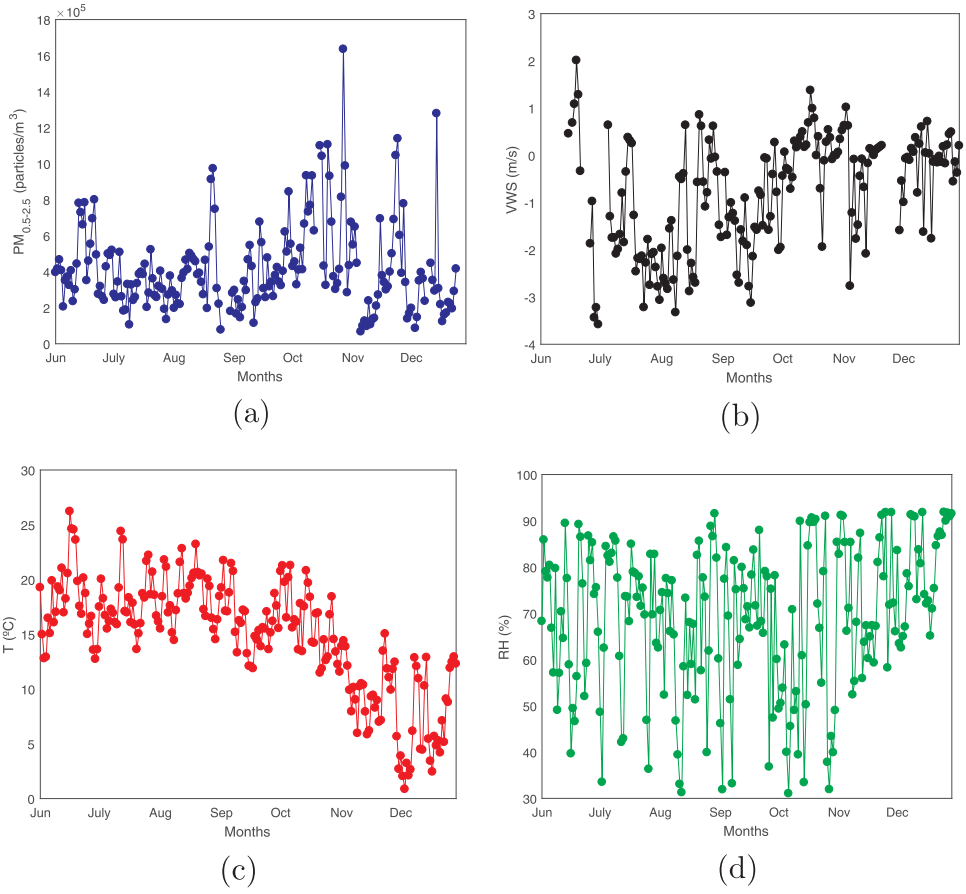

Fig. 4. Environmental parameters: (a) $PM_{0.5-2.5}$; (b) VWS; (c) T; (d) RH.

$$\Delta\lambda = \beta_0 + \beta_1 X_1 \beta_2 X_2 + ... \beta_n X_n \beta_{n-1} X_{n-1} \quad (5)$$

The stepwise method is exactly the same as for the MLR with the same criterion, which yields the Eq. (6):

$$\Delta\lambda_{MLRIT} = \beta_0 + \beta_1(PM_{0.5-2.5} \times VWS) + \beta 2(PM_{0.5-2.5} \times RH) + \beta 3(VWS \times RH) + \beta 4(RH \times T) \quad (6)$$

However the variables that maximize MLRIT are the same that do so for MLR, these no longer contribute independently to the output. Such model has the following statistical parameters: $r^2 = 0.279$, $adjr^2 = 0.228$ and $RMSE = 0.0042$. This model has a higher r^2 and $adjr^2$ and lower $RMSE$ than MLR model, as expected. The improvement of r^2 from MLR to MLRIT, near the double, shows the importance of interaction terms and the failure of simple linear models. Interaction terms have real physical meaning in the description of soiling, for instance, the interaction between $PM_{0.5-2.5}$ and VWS highlights the enhancement in soiling found at high levels of particulate matter and downward moderate winds.

It should be noted that r^2 value for MLRIT is close to the ones in [23] for an artificial neural network with one hidden layer having 5 neurons. But more on neural networks will be discussed afterwards.

Fig. 5 represents the scatter plots (colors representing intensities of $\Delta\lambda$), of the interaction variables presented in Eq. (6). It should be noted that all circles within Fig. 5 contain more than 50% of the points corresponding to $\Delta\lambda > 0.008$, which statistically ensures that these areas are the ones with the highest concentration of points representing situations where soiling increased from one day to the next.

It can be observed in Fig. 5a that most of the points corresponding to a substantial increasing in soiling are connected to downwards winds (magenta circle), however if there are more particles and the wind is blowing upwards (at a very low velocity) there can also be deposition, which demonstrates the importance of particle concentration. In Fig. 5b it can been seen that higher relative humidity is related to more deposition, as referred before, through an increased particle size and subsequent deposition [20], due to an increased electrostatic attraction or possible minimal dew formation, which allows for particles to be easier retained.

From Fig. 5c, it can be seen that the combination of downwards wind and high relative humidity may lead to higher particle deposition and consequently performance loss. Wind blowing downwards, together with possible particle hygroscopic growth enhances particle deposition (through increased particle adhesion). It can be seen that even for very low downward and upward winds there is deposition. This means that relative humidity is an extreme important factor, in this case, for soiling enhancement.

Fig. 5d shows a very interesting combination, which is that high air temperatures and relative humidity are somehow connected to increased soiling. This situation is probably representing what happens during Summer (when most of the times the soiling increased from day-to- day), when there may exist moderate temperatures and relative humidity. What can be possibly happening is during Summer there are normally higher temperatures compared to Fall, while there are more nights with higher relative humidity on Fall compared to Summer. This way, dew does not form so frequently during Summer, or it forms but at minimal amounts and dries faster, which can increase particle deposition, while during Fall, lower temperatures and possibly more frequently dew formation in larger amounts will not dry that fast, allowing surface cleaning. For higher clarity, the 3D scatter plot in Fig. 6 can be observed.

The upward wind data points were removed from the plot for better visualization. It is observed that most of the points related to a decrease of $\Delta\lambda$ are located in the bottom right corner, which corresponds to

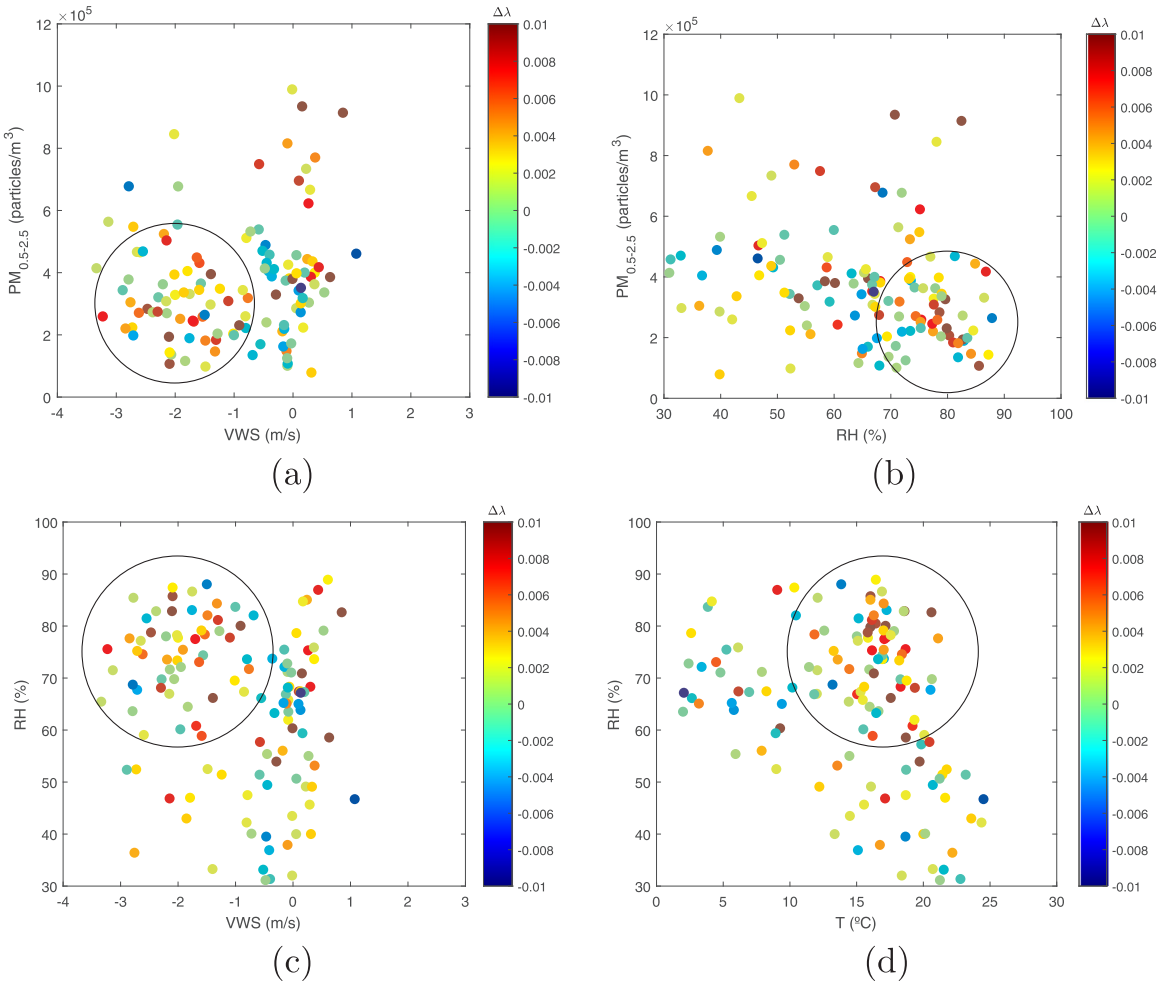

Fig. 5. Predictors effects between: (a) $PM_{0.5-2.5}$ and VWS; (b) $PM_{0.5-2.5}$ and RH; (c) VWS and RH; (d) T and RH.

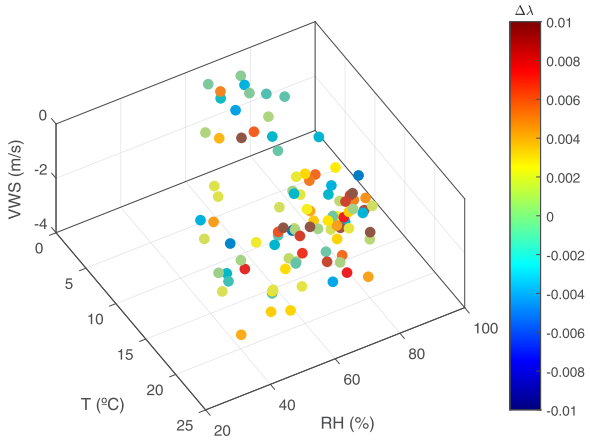

Fig. 6. Three dimensional scatter plot of predictors and output.

higher temperatures and relative humidity and moderate values of downwards wind speed. This summarizes what as been stated before in terms of environmental parameters.

It should be noted that MLRIT explains better the variation of the output, however it yields a poor result. It is known that this is a very complex problem to solve, however this study is important, because it shows unknown trends in the data and between variables, which can help in the future other researchers to achieve an analytical model. Next section will treat this problem with neural networks to access their potential in this field.

3.3. Neural Network

Artificial neural networks (ANN) have been vastly used in the last decade with different scopes [24–26] due to its potential to deal with highly complex problems, for which there is not yet an analytical solution. This seems to be one of those problems, where only trends could be understood on the data (which is also important). A single layer perceptron, see Fig. 7, is tested, which is a neural network with only one hidden layer. For more information on neural networks see [27].

The training algorithm chosen was the Levenberg-Marquardt [28].

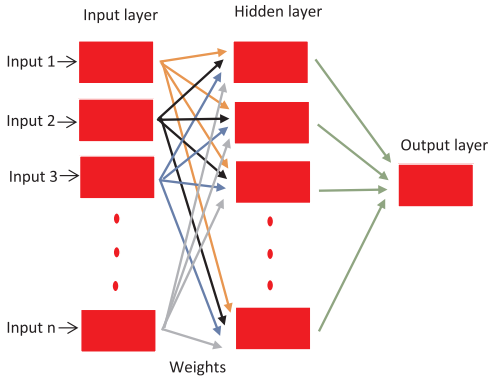

Fig. 7. ANN architecture.

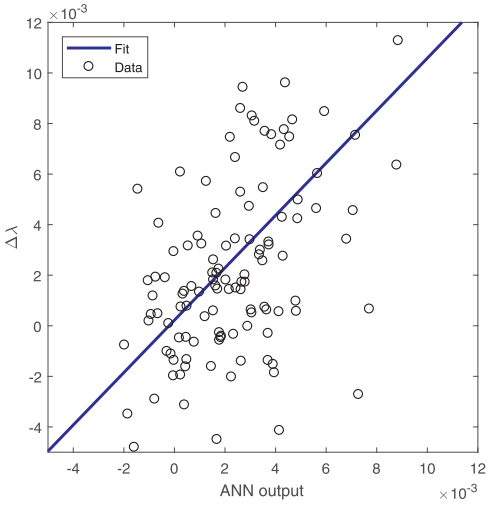

Fig. 8. ANN predictions and target output.

Table 1
Soiling index rates and associated statistical parameters.

	Jun	Jul	Aug	Sep
λ (%/month)	13.3	8.8	11.5	8.8
r^2	0.956	0.986	0.927	0.953
RMSE (%)	0.009	0.003	0.01	0.006

Table 2
Statistical parameters of models.

	MLR	MLRIT	ANN
r^2	0.150	0.279	0.629
RMSE	0.0045	0.0042	0.0037
MSE	2.03e−5	1.78e−5	1.40e−05

To find the optimum number of neurons in each hidden layer, the dataset was divided in two: one for designing purposes (90% of the data) and the other for calculating the mean square error, MSE, of those designs. The maximum number of neurons tested was 10, to avoid overfitting. Each design was tested 10 times [13] and MSE (the chosen performance index) calculated each time, using the testing dataset. The design with the lowest MSE was selected, to improve generalization for new data. For the hidden, layer a sigmoid function was selected, while for the output layer a linear one was used. It should be noted that inputs and outputs of ANN are the same as in for MLR and MLRIT. The results comparing the targets with the output from ANN are shown in Fig. 8:

Due to the lack of more extensive data series and additional variables in the model, like turbulence and confirmation of dew formation, it was not possible to increase the explained variability of the problem. Nevertheless, this is a fast process and gives better results than linear models. If there is not an analytical solution for this problem, ANN appears to be a promising tool, although there is the need of finding all the variables that somehow contribute to the solution Table 1.

3.4. Model comparison and discussion

It can be observed in Table 2 the statistical parameters chosen to evaluate the goodness of the fit for the different models.

From the most simple to the more complex model, it is stated an increase in r^2 and a decrease in both *RMSE* and *MSE* is shown, as expected. The simpler models, MLR and MLRIT, besides their low ability to explain the variability in the data, are important for a fundamental study in terms of basic relations and trends between the predictors and the output. MLRIT is important, because it shows how the predictors can be interlinked with each other and the effect on the output. ANN on the other hand do not serve to study the physical meaning behind the data, but it is instead a tool that can be used to solve complex problems. It was not possible to achieve higher r^2 values, although they are higher than the ones found, for instance, in [18]. Possibly more data points are required, for instance, to increase ANN learning skill, using more examples, but also because there are more variables that need to be introduced, like knowing exactly when dew and very light rain occurred, which can be very important for both cleaning or soiling increase, while atmospheric turbulence and convection may also play a role, as well as other variables. The time-scale, in which the variables and output is calculated, is related to the results, so there is a need for a deeper study of these topics.

4. Conclusions

This study contributes to enrich knowledge on the effect of soiling in the loss of reflectance of mirrors, which is connected to CSP technologies, and most specific to Fresnel and tower, since the reflectors are flat or nearly so. It should be noted that many more studies have been done regarding PV and therefore the effect of soiling in glass transmittance. That underscores the need for more studies of this kind. It should also be noted that this is the first paper, to the authors best knowledge, dealing with TraCS data and relating it with environmental parameters. It was possible to observe well defined soiling rates during Summer, as expected, and make a comparison between them and the ones from a PV system, as well as to detect trends between soiling increase/decrease and environmental behaviour. Soiling prediction was also made using artificial neural networks, however better results can be obtained if more data, variables and different time-scales are used.

Acknowledgments

Ricardo Conceição acknowledges the FCT scholarship with the reference SFRH/BD/116344/2016. All authors are grateful to the Renewable Energies Chair and the Institute of Earth Sciences, University of Évora, for supporting this work. Hugo Silva acknowledges the support from the project DNI-A with the reference ALT20-03-0145-FEDER-000011. This work was co-funded by the European Union, through the European Regional Development Fund, framed in COMPETE 2020 (Operational Programme Competitiveness and Internationalisation) through ICT (UID/GEO/04683/2013) with reference POCI-01-0145-FEDER-007690. All authors acknowledge Phillip Bellmann and Dr. Fabian Wolfertstetter for their contribution on the TraCS assembly and discussions about its performance, as well as CSP Services for providing the sensor.

References

[1] H.P. Garg, Effect of dirt on transparent covers in flat-plate solar energy collectors, Sol. Energy 15 (1974) 299–302.
[2] M. El-Shobokshy, F.M. Hussein, Effect of dust with different physical properties on the performance of photovoltaic cells, Sol. Energy 51 (6) (1993) 505–511.
[3] A.M. El-Nashar, Effect of dust deposition on the performance of a solar desalination plant operating in an arid desert area, Sol. Energy 75 (5) (2003) 421–431.
[4] S. Bouaddi, A. Ihlal, A. Fernández-García, Soiled CSP solar reflectors modeling using dynamic linear models, Sol. Energy 122 (2015) 847–863.
[5] S. Bouaddi, A. Ihlal, A. Fernández-García, Comparative analysis of soiling of CSP mirror materials in arid zones, Renew. Energy 101 (2017) 437–449.
[6] R. Conceição, H. Silva, J. Mirão, M. Gostein, L. Fialho, L. Narvarte, M. Collares-Pereira, Saharan dust transport to Europe and its impact on photovoltaic performance: a case study of soiling in Portugal, Sol. Energy 160 (2018) 94–102.
[7] R. Conceicão, H.G. Silva, J. Mirão, M. Collares-Pereira, Organic Soil-ing: The Role of Pollen in PV Module Performance Degradation, 2018, 1-13.
[8] E.P. Roth, R.B. Pettit, The effect of soiling on solar mirrors and techniques used to maintain high reflectivity, Sol. Mater. Sci. (1980) 199–227.
[9] R. Pettit, J. Freese, Wavelength dependent scattering caused by dust accumulation on solar mirrors, Sol. Energy Mater. 3 (1–2) (1980) 1–20.
[10] D.J. Griffith, L. Vhengani, M. Maliage, Measurements of mirror soiling at a

candidate CSP site, Energy Proc. 49 (2013) 1371–1378.
[11] A.A. Merrouni, F. Wolfertstetter, A. Mezrhab, S. Wilbert, R. Pitz-Paal, Investigation of soiling effect on different solar mirror materials under moroccan climate, Energy Proc. 69 (2015) 1948–1957.
[12] P. Bellmann, F. Wolfertstetter, H.G. Silva, R. Conceicao, Comparative modelling of optical soiling losses for CSP and PV devices in regard to gravimetric density, Sol. Energy (2018) (In preparation).
[13] M. Torres-Ramírez, D. Elizondo, B. García-Domingo, G. Nofuentes, D.L. Talavera, Modelling the spectral irradiance distribution in sunny inland locations using an ANN-based methodology, Energy 86 (2015) 323–334.
[14] F. Wolfertstetter, K. Pottler, A.A. Merrouni, A. Mezrhab, R. Pitz-paal, A novel method for automatic real-time monitoring of mirror soiling rates, Sol. Conc. Sol. Power Chem. Energy Syst. (2012) 2–5.
[15] F. Wolfertstetter, K. Pottler, N. Geuder, R. Affolter, A.A. Merrouni, A. Mezrhab, R. Pitz-Paal, Monitoring of mirror and sensor soiling with TraCS for improved quality of ground based irradiance measurements, Energy Proc. 49 (2013) 2422–2432.
[16] H.G. Silva, R. Conceição, M.D. Wright, J.C. Matthews, S.N. Pereira, D.E. Shallcross, Aerosol hygroscopic growth and the dependence of atmospheric electric field measurements with relative humidity, J. Aerosol Sci. 85 (2015) 42–51.
[17] R. Conceição, H. Silva, A. Bennett, R. Salgado, D. Bortoli, M. Costa, M. Collares Pereira, High-Frequency Response of the Atmospheric Electric Potential Gradient Under Strong and Dry Boundary-Layer Convection, Boundary-Layer Meteorol.
[18] B. Guo, W. Javed, B. Figgis, Modeling of PV Soiling as A Function of Environmental Variables, Soiling E . PV Modul. Dubai, April 5-7, 2016 157 (August) (2016) 1–23.
[19] A.K. Kamra, C.G. Deshpande, V. Gopalakrishnan, Effect of relative humidity on the electrical conductivity of marine air, Q. J. R. Meteorol. Soc. 123 (1997) 1295–1305.
[20] G. Hänel, Influence of relative humidity on aerosol deposition by sedimentation, Atmos. Environ. 16 (11) (1982) 2703–2706.
[21] G. Ahmadi, S. Guo, X. Zhang, Particle adhesion and detachment in turbulent flows including capillary forces, Part. Sci. Technol. 25 (1) (2007) 59–76.
[22] B. Guo, W. Javed, B.W. Figgis, T. Mirza, Effect of dust and weather conditions on photovoltaic performance in Doha, Qatar, 2015 1st Work. Smart Grid Renew. Energy, SGRE 2015.
[23] W. Javed, B. Guo, B. Figgis, Modeling of photovoltaic soiling loss as a function of environmental variables, Sol. Energy 157 (2017) 397–407.
[24] S. Pulipaka, R. Kumar, Power prediction of soiled PV module with neural networks using hybrid data clustering and division techniques, Sol. Energy 133 (2016) 485–500.
[25] S. Pulipaka, F. Mani, R. Kumar, Modeling of soiled PV module with neural networks and regression using particle size composition, Sol. Energy 123 (2016) 116–126.
[26] B. Laarabi, O. May Tzuc, D. Dahlioui, A. Bassam, M. Flota-Bañuelos, A. Barhdadi, Artificial neural network modeling and sensitivity analysis for soiling effects on photovoltaic panels in Morocco, Superlattices Microstruct.
[27] S.A. Kalogirou, Artificial neural networks in renewable energy systems applications: a review, Renew. Sustain. Energy Rev. 5 (4) (2001) 373–401.
[28] D.W. Marquardt, An Algorithm for Least-Squares Estimation of Nonlinear Parameters, J. Soc. Indust. Appl. Math. 11 (2).